7

The Nile Basin sediment loss and degradation, with emphasis on the Blue Nile

Tammo S. Steenhuis, Zachary M. Easton, Seleshi B. Awulachew, Abdalla A. Ahmed, Kamaleddin E. Bashar, Enyew Adgo, Yihenew G. Selassie and Seifu A. Tilahun

Key messages

- Run-off and erosion are spatially distributed in the landscape. Contrary to the prevailing consensus, the steep slopes in well-established agricultural watersheds in humid climates are usually not the main sources of sediment.
- Most run-off and sediments originate from both the severely degraded areas with shallow topsoils and points near a river when they are becoming saturated, around the middle of the rainy phase of the monsoon. Degraded areas that are bare deliver greater amounts of sediment than the saturated areas that are vegetated.
- Two simulation models (SWAT-WB and the water balance type model), adapted to the Ethiopian Highlands, widely ranging in complexity, were able to simulate the available sediment concentrations equally well. This illustrates the point that conceptual correctness is more important than complexity in simulating watersheds.
- Gully formation is an important source of sediment in the Blue Nile Basin. Sediment concentration can be up to an equivalent of 400 t ha^{-1} in the watershed. Although gullies are formed on the hillsides, the largest gullies of up to 5 m depth and 10 m width are formed in the periodically saturated and relatively flat lands near the river.
- On average, the annual sediment loss in the Blue Nile Basin at the border with Sudan is 7 t ha^{-1} and is equivalent 0.5 mm of soil over the entire basin. Although this seems to be relatively small, it is an enormous amount of sediment for the Rosaries reservoir and, consequently, its capacity to store water has been decreased significantly since 1966 when it was completed.

Introduction

High population pressure, poor land-use planning, over-dependency on agriculture as a source of livelihoods and extreme dependence on natural resources are inducing deforestation, over-grazing, expansion of agriculture to marginal lands and steep slopes, declining agricultural

productivity and degradation of the environment. Poor agricultural and other practices affect run-off characteristics resulting in increased erosion and siltation and reduced water quality in the BNB (Awulachew *et al.*, 2008). FAO (1986) estimates an annual loss of over 1.9 billion tonnes of soil from the Ethiopian Highlands. Only approximately 122 million tonnes reach the Ethiopia border (Ahmed and Ismail, 2008). Erosion from the land surface occurs in the form of sheet erosion, rill and inter-rill erosion, or gully erosion, part of which is delivered to rivers. This, together with deposition of erosion from in-stream beds and banks of rivers, constitutes the sediment load in the river (Awulachew *et al.*, 2008). According to Hydrosult *et al.* (2006), the Ethiopian plateau is the main source of the sediment in the Blue Nile system. The main area of sheet erosion is within the Ethiopian Highlands. Some sheet erosion occurs within Sudan, mainly on and around the rock hills, which have become devoid of vegetative cover. Most of this is deposited on the foot slope and does not enter the drainage system. Those streams reaching the river during the rainy season can carry high sediment concentrations. The eroded and transported sediment ultimately reaches Sudan, and can cause significant loss of reservoir volume and transmittance capacity in irrigation canals. In fact, some sediment from the Highlands is transmitted to the Aswan High Dam as suspended sediment. As a result, we have focused on the study of erosion, sedimentation and understanding the impacts of inter-vention measures in the BNB (including from the Ethiopian Highlands to the Roseires reservoir in Sudan).

Modelling of the processes governing erosion and sedimentation can further help our understanding of the basin-wide issues in terms of the critical factors controlling erosion and associated sediment transport. However, sediment modelling on a daily or weekly basis in Ethiopia has generally not been very successful, because the underlying hydrological models have not predicted run-off well (e.g. the Agricultural Non-Point Source Pollution, or AGNPS, model; Haregeweyn and Yohannes, 2003; Mohammed *et al.*, 2004), Soil and Water Assessment Tool (SWAT; Setegn *et al.*, 2008) and Water Erosion Prediction Project (WEPP; Zeleke, 2000). Various modelling approaches have been attempted with a limited degree of success because of an ineffective ability to link erosion and sediment transport to the correct hydrological process. We present an in-depth analysis of the various landscape sediment sources to better understand the erosion–sediment transport relationship of the BNB watershed. Unfortunately, there is a general lack of sediment data, particularly time series of sediment concentrations in the vari-ous reaches of the basin. We first explore which data are available from routine measurements and in experimental watersheds followed by a description of how we have modelled these data using the hydrology models presented in Chapter 6; finally, we discuss the implication of our findings on structural and non-structural practices.

Available sediment concentration data

Similar to the rainfall run-off studies discussed in Chapter 6, primary and secondary data are collected routinely at sub-basin level on tributary rivers and the main stream of the Blue Nile; additional data on quantities of sediment can be obtained at the Ethiopia Sudan border (El Diem station) where the Roseires reservoir has been trapping sediment for over 40 years. Finally, data on sediment concentration are available from experimental watershed stations of the Soil Conservation Reserve Program (SCRP; Herweg, 1996), which have long records (such as from Anjeni, Maybar and Andit Tid), while shorter records are available from the Debre-Mawi and Koga watersheds.

Routine collection of sediment data

An examination of the sediment stations available from the Ministry of Water Resources (MoWR) in Ethiopia shows that there are altogether 45 stations in the Abbay Basin. However, most of these have only very sporadic measurements and most are related to periods during which stage, discharge relationships were developed or revisions to such relationships were made. A consolidated list of stations with data records for the Abbay is provided by Awulachew et al. (2008).

Preliminary analyses of the routinely measured data show that sediment peaks during the rainy season, particularly in July. However, almost no sediment is measured in the streams in the dry season. The annual sediment concentration (sediment weight per volume of water) measured in mg l^{-1} shows the highest sediment concentrations from June to September, generally peaking in July, while rainfall and run-off peaks occur in August.
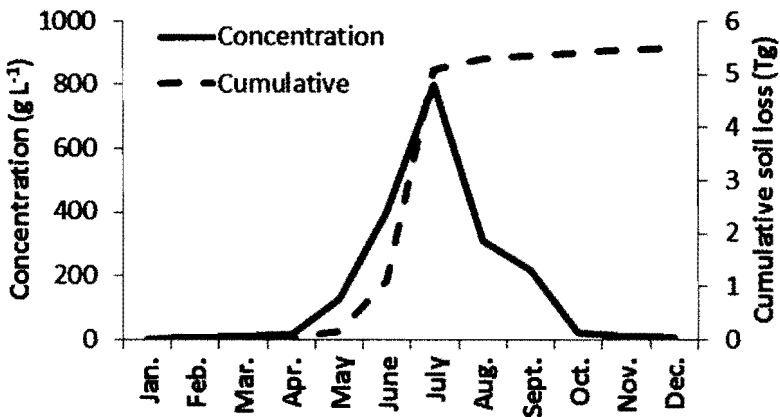

Figure 7.1 Typical monthly sediment concentrations, cumulative sediment load over time at Ribb at Addis Zemen station, a tributary of Lake Tana and the Blue Nile

Figure 7.1 illustrates a typical sediment concentration time series for the Ribb River at Addis Zemen in the Lake Tana watershed. The river is a medium-sized watershed tributary, with a drainage area of about 1600 km². An important implication is that the sediment rating curve established on flow volume or river stage alone cannot provide accurate estimation of sediment yield. Rainfall and run-off are the driving factors for the onset of the erosion process. However, timing of rainfall, land use and land cover have a major influence on the erosion process (Ahmed and Ismail, 2008).

Data derived from trapping of sediments in reservoirs

Accumulation of sediment in a reservoir can be used to indicate the severity of the land degradation, erosion, sediment transport and minimum yield at that particular point. The Roseires reservoir is of particular interest as it acts as the sediment sink for the entire Ethiopian Highlands. The annual amount of sediment delivered by the Blue Nile at the entrance of the

Roseires reservoir is, on average, 122 million tonnes per year (t yr⁻¹). The bed load is less than 10 per cent. The coarser sand is deposited in the upper portion of the Blue Nile near the Ethiopia–Sudan border, while the lighter sediment is carried by the flow downstream. The suspended sediment load distribution is 30 per cent clay, 40 per cent silt and 30 per cent fire sand (Ahmed and Ismail, 2008).

Bashar and Khalifa (2009) used bathymetric surveys conducted in 1976, 1981, 1985, 1992, 2005 and 2007 to assess the rate of sedimentation in the Roseires reservoir. In order to calculate the amount of sediment deposited, the design storage capacity in 1966 for the different reservoir levels was taken as a baseline. The reservoir storage capacity as a function of the reservoir for the years that the bathymetric surveys were taken is depicted in Figure 7.2. In the 41 years of operation (1966–2007), the maximum storage capacity at 481 m decreased from 3330 million to 1920 million m³. This represents a loss of storage capacity of 1410 million m³, and thus only 60 per cent of the initial storage is still available after 41 years. The reservoir is currently filled with sediment up to the 470 m level (Figure 7.2). The total amount of sediment delivered over the 41 years to the Roseires reservoir is approximately 5000 million tonnes, or 3000 million m³. This represents a decrease of twice the storage capacity in the reservoir, since the reservoir operation rule maintains that only the end of the rainy season flow is stored, which is when the sediment concentration is smallest (Figure 7.1).
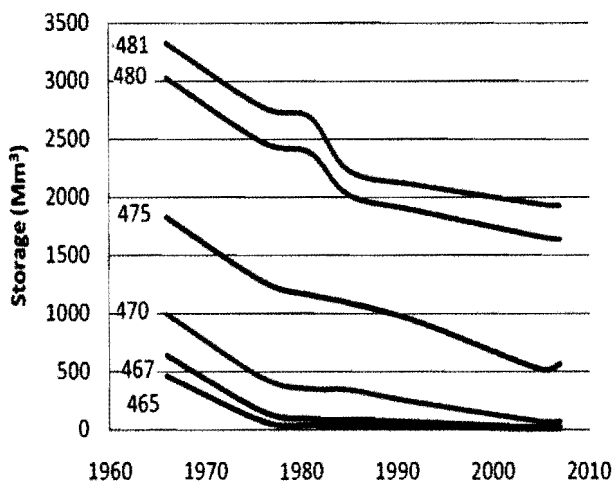

Figure 7.2 Variation of storage with time at various reservoir levels (m) in the Roseires reservoir
Source: Bashar and Khalifa, 2009

Upland and gully erosion in micro watersheds

Since the establishment of the micro-watersheds by the SCRP in 1981, high-resolution data on climate, hydrology and suspended sediment, from both rivers and test plots, have been collected. Hence, an expansive database has been established that has served as a data source for understanding and quantifying erosion processes and for validating models. The Anjeni, Andit Tid and Maybar watersheds are located near or in the BNB and have over 10,000 combined observations.
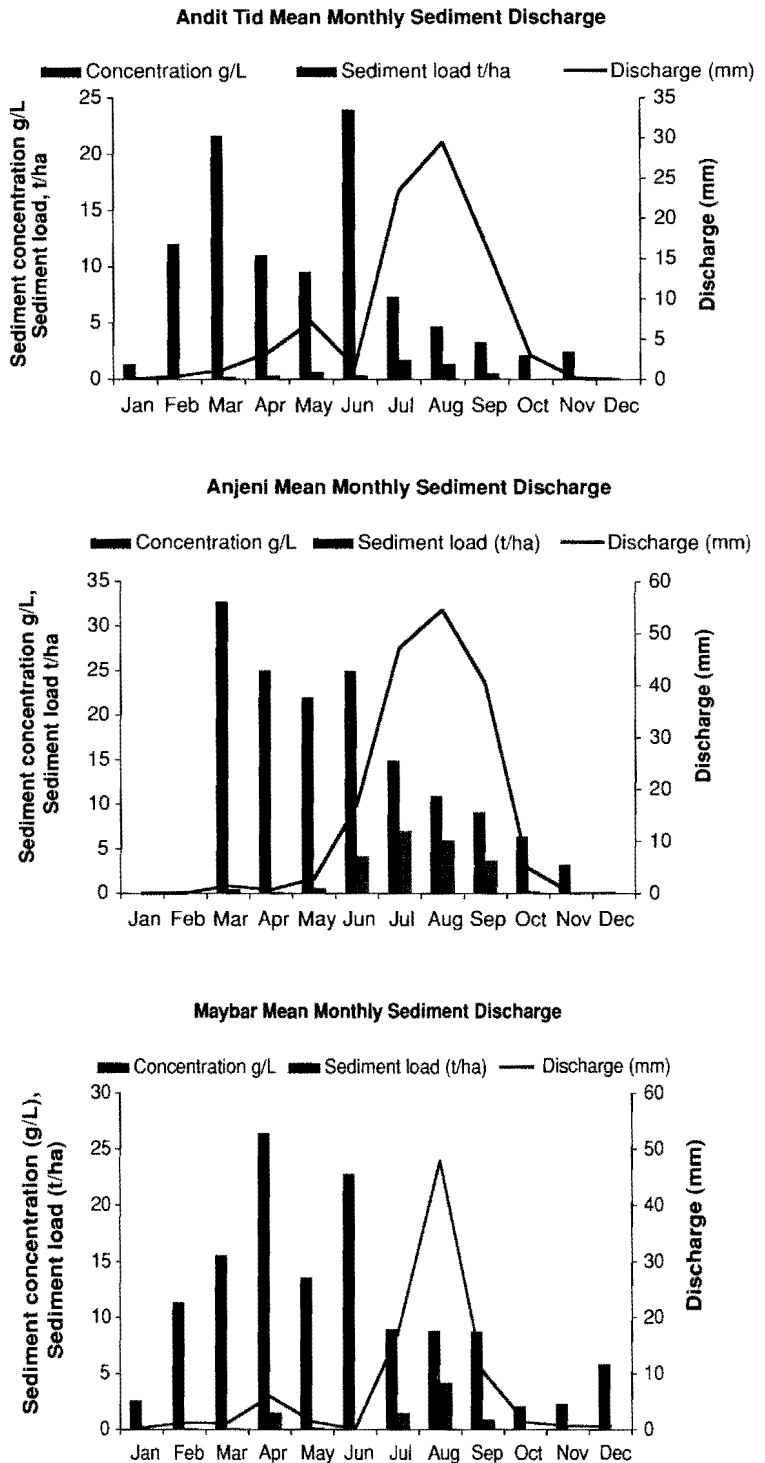
Andit Tid Mean Monthly Sediment Discharge

Anjeni Mean Monthly Sediment Discharge

Maybar Mean Monthly Sediment Discharge

Figure 7.3 Mean monthly concentration of sediment in the SCRP watersheds

Both sediment concentration and discharge data are available for each measurement with a resolution of 10 minutes during run-off events. Based on these measurements, annual sediment yields during run-off events were 5.4, 22.5 and 8.8 t ha^{-1}·yr^{-1} for Andit Tid, Anjeni and Maybar, respectively (Guzman, 2010). During the main rainy season, there was a decrease in average sediment concentration over the course of the season (Figure 7.4). This decrease was less noticeable at the Maybar site than at the other two sites, possibly caused by the more variable year-to-year fluctuations in precipitation and discharge for the Maybar watershed (Hurni *et al.*, 2005). Unfortunately, a simple sediment rating curve could not be developed for these water-sheds either. The maximum correlation coefficient did not exceed 0.22 for any watershed when all discharge–sediment data were used. These small watersheds offer an ideal opportunity to investigate the reason for the non-uniqueness in the sediment rating curve. This is best illus-trated in Anjeni where the average concentrations are calculated over daily periods. Two storms are depicted, one in the beginning of the short rainy season (24 April 1992; Figure 7.4a) and the other, later in the rainy season (19 July 1992; Figure 7.4b; Tilahun *et al.*, 2012).
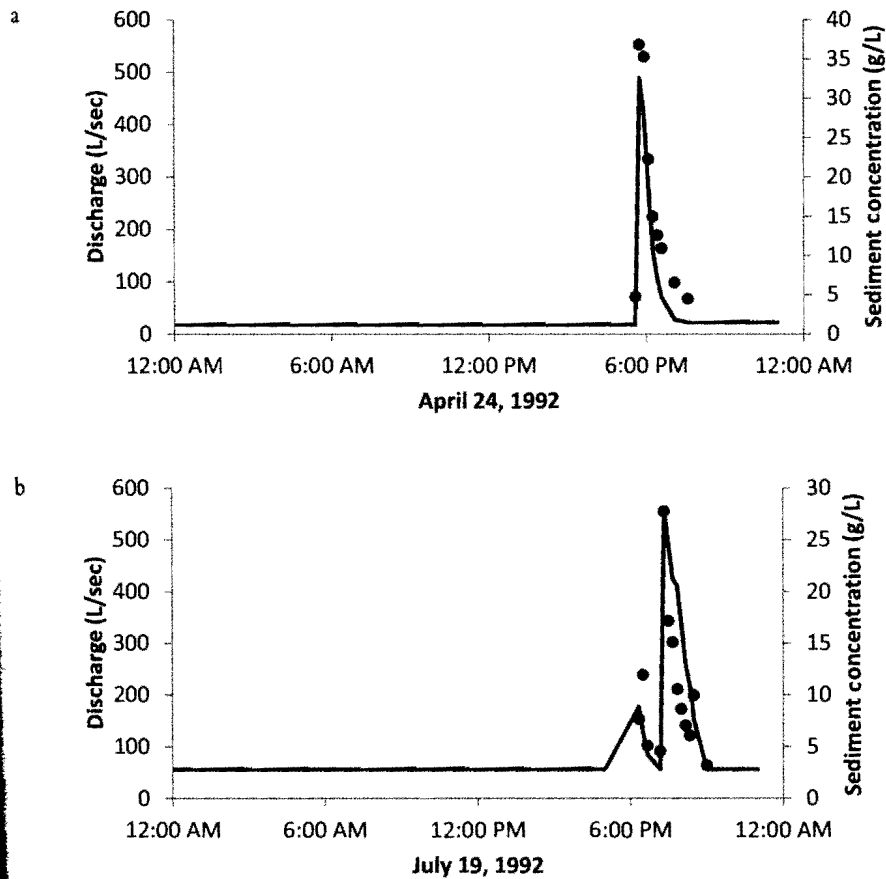

Figure 7.4 Measured discharge (solid line) and sediment concentration (closed circles) for the Anjeni watershed on (a) 24 April 1992 and (b) 19 July 1992

The surface run-off for both events is similar with a peak run-off of 400–500 l s^{-1}. The duration of the run-off event was approximately 2 hours. The peak sediment concentrations were nearly the same, around 30–35 g l^{-1}. Baseflow discharge is low during the beginning of the rainy season (around 10 l sec^{-1} for April or equivalent to 0.8 mm day^{-1} over the whole watershed). Baseflow increases during the rainy season and is approximately 50 l sec^{-1} (equivalent to 4.0 mm day^{-1}) in July. Despite the similar surface run-off characteristics the total flows for April and July were 2400 and 6500 m^3, respectively. The averages of the daily sediment concentration can be obtained by dividing the load by the total flow, resulting in a concentration of 11.3 g l^{-1} for the April storm and 4.4 g l^{-1} for the July storm. In essence, the baseflow dilutes the peak storm concentration when simulated on a daily basis later in the rainy season. Thus, since the ratio of the baseflow to surface run-off is increasing during the wet season the temporally averaged concentration is decreasing. Figure 7.5 shows this clearly for the Anjeni watershed. Therefore, it is important to incorporate the contribution of baseflow in the prediction of sediment concentrations.
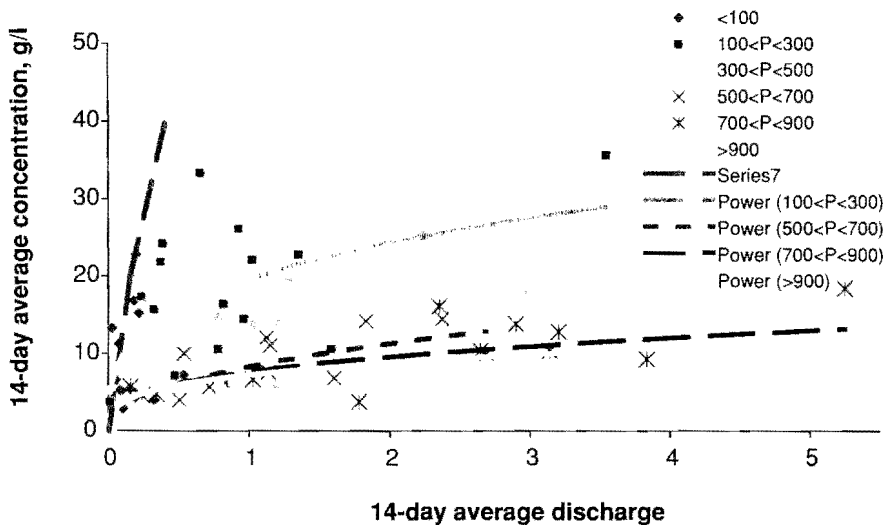

Figure 7.5 Stratified biweekly storm concentration versus discharge for Anjeni

Note: Symbols indicate the amount of cumulative effective precipitation, P, since the beginning of the wet period: diamonds, P<100 mm; squares, 100<P<300 mm; triangles, 300<P<500 mm; crosses, 500<P<700 mm; stars, 700<P<900 mm; circles, P>900 mm

Gully erosion

Gully formation and upland erosion were studied in the Debre-Mawi watershed south of Lake Tana by Abiy (2009), Tebebu *et al.* (2010) and Zegeye *et al.* (2010). We selected one of the gullies (Figure 7.6a, b) with a contributing area of 17.4 ha. According to farmers' interviews through the AGERTIM (Assessment of Gully Erosion Rates through Interviews and Measurements method; Nyssen *et al.*, 2006), the gully erosion started in the early 1980s, which corresponds to the time when the watershed was first settled and the indigenous vegetation on the hillsides

was converted gradually to agricultural land. Almost all farmers agreed on the incision location of the current gully and confirm that the locations of the two gully incisions were related to three springs on the hill slope. Erosion rates for the main stem and two branches are given in Table 7.1. Walking along the gully with a Garmin GPS with an accuracy of 2 m, gully boundaries were determined before the rainy season in 2008 (indicated as 2007 measurement) and after the rainy season on 1 October (the 2008 measurement). The increase in the main stem erosion rate (gully C) from an average of 13.2 to 402 t ha^{-1} yr^{-1} from 1980 to 2007 is due to the recently enlarged and deepened gully at the lower end (Figure 7.6b). Although not shown in the table, our measurements showed that from 2005 to 2007, the gully system increased from 0.65 to 1.0 ha, a 54 per cent increase in area. In 2008, it increased by 43 per cent to cover 1.43 ha from the year before. This is a significant amount of loss of land in a 17.4 ha watershed. The increase in rate of expansion of gully formation 20–30 years after its initial development is in agreement with the finding of Nyssen *et al.*, 2008 in the May Zegzeg catchment, near Hagere Selam in the Tigray Highlands, at which the gully formation follows an S shape pattern. Although it is slow in the beginning and end, there is a rapid gully formation phase after 20–30 years after initialization of the gully and then erosion rates decrease again.
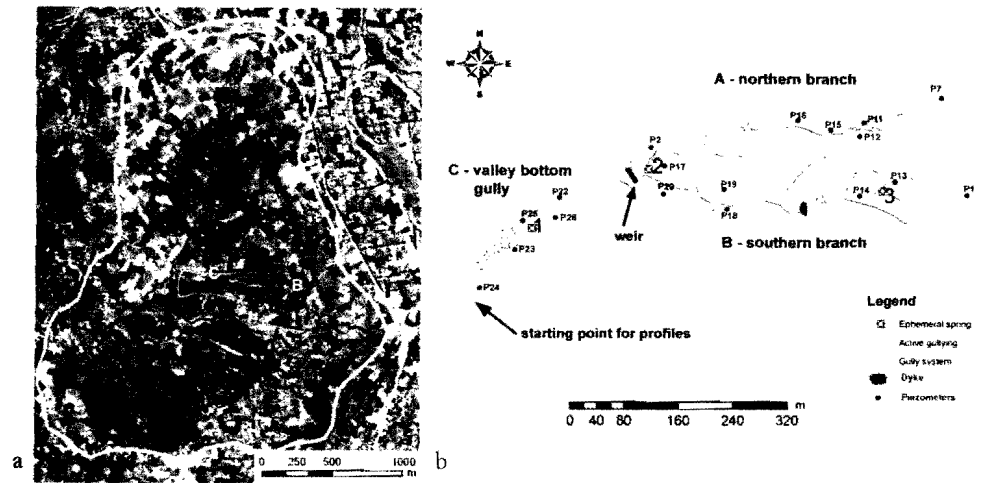

Figure 7.6 Map of the Debra-Mawi watershed (a) with the gully area outlined in red and (b) the Debre-Mawi gully extent generated by hand-held GPS tracking; active erosion areas are indicated by triangles. Ephemeral springs and piezometer locations are shown as well

Table 7.1 Erosion losses for gullies A, B and C. Erosion rates calculated from the gullies are then distributed uniformly over the contributing area

Gully location	Soil loss		
	1980–2007 (t ha^{-1} yr^{-1})	2007–2008 (t ha^{-1} yr^{-1})	2007–2008 (cm yr^{-1})
Branches (gullies A and B)★	17.5	128	1
Main stem (gully C)	13.2	402	3
Total	30.7	530	4

Note: ★The calculated erosion rates for gullies A and B were nearly identical, and are thus presented in aggregates

In order to investigate the cause of the gully erosion, 24 piezometers were installed at depths up to 4 m in the gully bottom, as well as in the gully's contributing area (Figure 7.6b; Tebetu *et al.*, 2010). The gully is very active in a few areas as indicated by the red triangles in Figure 7.6b. Active widening of the gully occurs when the water table is above the gully bottom. This is best illustrated in the large gully near the valley bottom (Figure 7.6b). The depth of the gully (Figure 7.7a) and the corresponding widths (Figure 7.7b) are depicted before the 2007 and after the 2008 rainy seasons for the area of the valley bottom as a function of the distance from the point where this gully joins the main branch. The average water table depths for adjacent piezometers (from bottom to top, P24, P23, P22, P26 and P17) are shown as well, and indicate that the valley bottom is saturated, while further uphill the water table is below the gully bottom. During the 2008 rainy season the gully advanced up the hill, past the 187 m point (Figure 7.7a) and increased up to 20 m in the top width (Figure 7.7b). In this region, the water table was near the surface and approximately 4 m above the gully bottom (Figure 7.7a). This means that under static conditions the pore water pressure near the gully advance point is 4 m, which might be sufficient to cause failure of the gully wall.

The piezometers P24 and P26 at 244 and 272 m indicate that the water table is at the surface (Figures 7.6 and 7.7), but that the gully is not incised as yet (Figure 7.7a). The area is flatter and, in the past, the sediment had accumulated here. It is likely that over the next few years the head wall will rapidly go uphill in these saturated soils. At the 323 and 372 m points the water table is below the bottom of the 4 m long P17 piezometer, and thus below the bottom of the gully. Here the gully is stable despite its 3 m depth.

Upland erosion

The second watershed was used to study upland erosion (rill and inter-rill erosion) processes in cultivated fields. The location of the upland site relative to the gully site is given in Figure 7.1. Soils consisted of clay and clay loam, and land use/land cover was similar to the gully site.

For determining rill erosion, 15 cultivated fields were selected in the contributing area, representing a cumulative area of 3.6 ha. These fields were classified into three slope positions: upslope (slope length of 100 m), mid-slope (slope length of 250 m) and toe-slope (slope length of 100 m). A series of cross-slope transects were established with an average distance of 10 m between two transects, positioned one above another to minimize interference between transects. During the rainy season, each field was visited immediately after the rainfall events in July and August, when the peak rainfall occurred. During these visits the length, width and depth of the rills were measured along two successive transects. The length of a rill was measured from its upslope starting point down to where the eroded soil was deposited. Widths were measured at several points along a rill and averaged over the rill length (Herweg, 1996). From these measurements, different magnitudes of rill erosion were determined, including rill volumes, rates of erosion, density of rills, area impacted by the rills, and the percentage of area covered by the rills in relation to the total area of surveyed fields (Herweg, 1996; Bewket and Sterk, 2005). The average upland erosion of the 15 agricultural fields is 27 t ha^{-1} over the 2008 rainy season in the Debre-Mawi watershed (Zegeye *et al.*, 2010). The lower watersheds had significantly greater soil erosion and greater area covered by rills than either the middle watershed or the upper watershed, which had the least of both (Table 7.2). It is hypothesized that this is related to the greater amount of run-off produced on the lower slopes (Bayabil *et al.*, 2010) causing the greater volume of rills. In addition, the Teff plots had the greatest density of rills, possibly caused by the repeated cultivation of the field and compaction of the soil by livestock traffic before sowing, and possibly because of the reduced ground cover from the later planting date for Teff
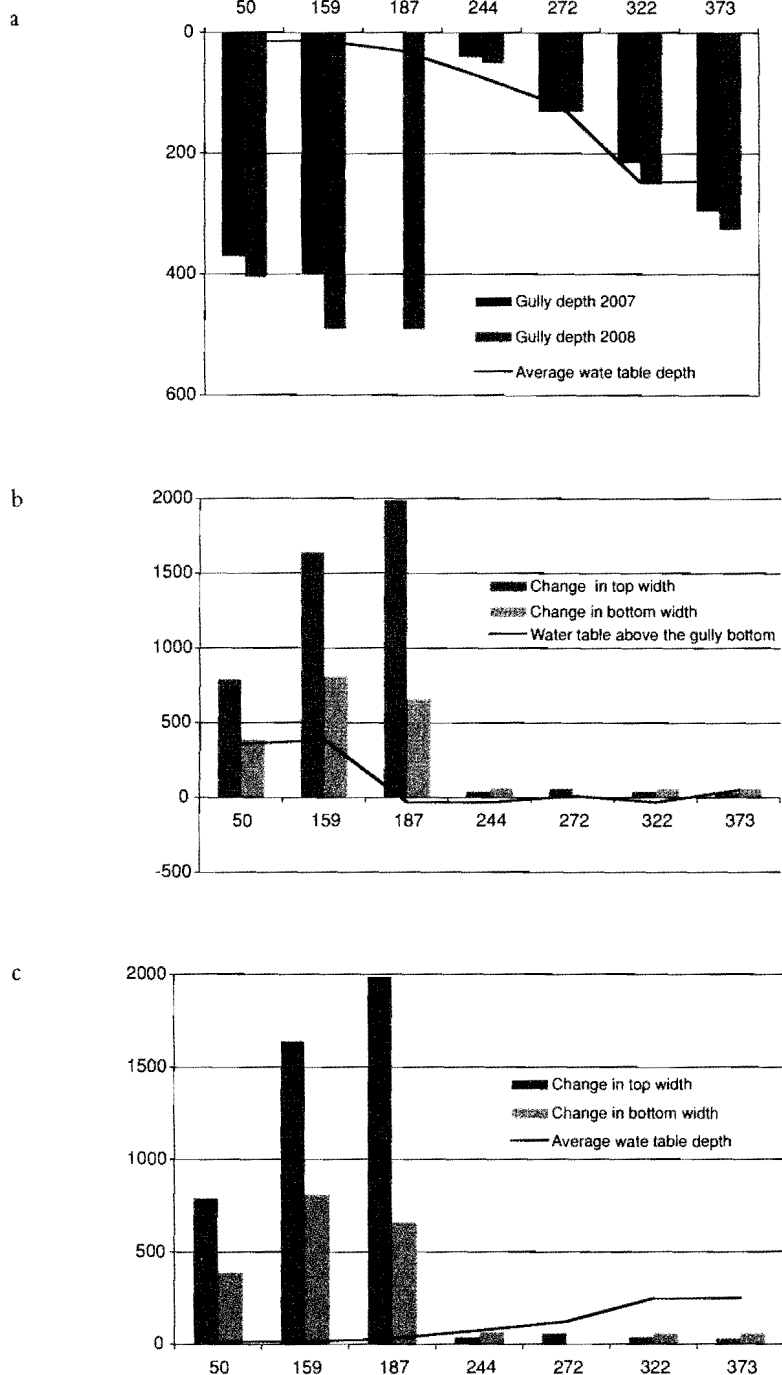
Figure 7.7 (a) Average water table and gully depths (m) before and after the 2008 rainy season for the main stem (gully C) using the soil surface as a reference elevation point, and (b) change in top and bottom widths (m) of the gully and average water table depth (m) above the gully bottom

(Zegeye *et al.*, 2010).The erosion is greatest at the end of June when the soil is loose and dry, making it easy to erode as rills (Bewket and Sterk, 2005). In late August, the rills degrade giving an apparent negative soil loss. At this time, the plant cover is established possibly reducing soil losses.

Table 7.2 Soil loss, area affected, rill density and slope percentage for the three different slope positions

Slope position	Slope (%)	Soil loss (t ha⁻¹)	Area of actual damage (m² ha⁻¹)	Rill density (m ha⁻¹)
Down slope	14a	34a*	884a	4469a
Mid-slope	10b	23b	662b	2860b
Upslope	9b	8c	256c	1029c

Note: *Means followed by different letters (a,b,c) within columns are significantly different at $\alpha = 0.05$

A comparison of the gully and upland erosion rates in the Debre-Mawi watershed indicates that the soil loss rate of the gully system is approximately 20 times higher than the erosion rates for the rill and inter-rill systems.While significantly lower than gully erosion, rill erosion is still nearly four times greater than the generally accepted soil loss rate for the region and thus cannot be ignored in terms of agricultural productivity and soil fertility. However, if reservoir siltation and water quality of Lake Tana and the Blue Nile constitute the primary impetus for soil conservation, gully erosion has far greater consequences.

Simulating erosion losses in the Blue Nile Basin

Schematization of the Blue Nile Basin for sediment modelling

To better understand the issues and processes controlling sediment, the BNB was divided into a set of nested catchments from micro-watershed to basin level that include micro- watershed level, watershed and small dam level, sub-basins and major lakes, basin outlet and a large reservoir (Awulachew *et al.*, 2008). In this section, we discuss some of the methods and models to predict erosion and sediment loads.We will start with the simple Universal Soil Loss Equation (USLE) and end with the more complicated SWAT-WB model.

Universal Soil Loss Equation

The simplest method to predict the erosion rates is using USLE, originally developed empirically based on a 72.6 m long plot for the United States east of the 100th meridian. It has been adapted to Ethiopian conditions using the data of long-term upslope erosion data of the SCRP sites of Mitiku *et al.* (2006). More recently, Kaltenrieder (2007) adapted USLE for Ethiopian conditions to predict annual soil losses at the field scale. The erosion data set collected by Zegeye *et al.* (2010) offers an ideal opportunity to check the modified USLE. The predicted erosion rate was calculated assuming that 25 per cent of the erosion was splash erosion. The predicted and observed erosion rates for the individual plots in the Debre-Mawi watershed (described above) are shown in Figure 7.8.Although USLE seems to predict the general magnitude of the plot-scale erosion well, it does not include erosion due to concentrated flow
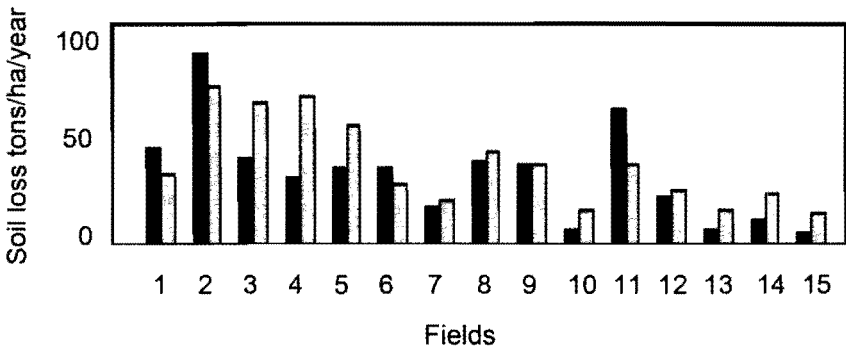
Figure 7.8 Comparison of modified USLE for Ethiopia and observed soil losses in the Debra-Mawi watershed. Observed soil loss is indicated by black bars and predicted loss by grey bars

channels and gullies (Capra *et al.*, 2005), which is another reason for not using USLE predictions without field verification.

Simple erosion model

We can use the simple model presented in Chapter 6 for predicting sediment concentrations and loads by assuming that baseflow and interflow are sediment-free and only surface run-off mobilizes sediment. If we assume that the velocity of the water (Hairsine and Rose, 1992) is linearly related to the concentration in the water, it is possible to predict the concentration of the sediment (Tilahun *et al.*, 2012):

$$C_t = \frac{a_s A_s Q_{s_t}^{1.4} = a_d A_d Q_{d_t}^{1.4}}{A_s Q_{s_t} + A_d Q_{d_t} + A_h \left(Q_{b_t} + Q_{I_t}\right)}$$

where C_t is the sediment concentration, A is the fraction in the watershed area that is saturated (s), degraded (d) or hillsides (h); the constant a represents the sediment and watershed characteristics for the saturated area (s) and degraded areas (d); and Q is the discharge per unit area at time t from either the saturated area (s) or degraded area (d) as overland flow or as subsurface flow from the hillside as baseflow (B) and as interflow (I).

Thus there are only two calibration parameters, one for each source area, that determine contribution to the sediment load of the source area at the outlet of the watershed. Although it is recognized that by incorporating more calibration parameters, such as plant cover, or soil type for the different areas, we might obtain a better agreement between observed and predicted sediment yield, the current methods seem to provide a reasonably accurate prediction of sediment yield, as shown in Figure 7.9. Note that in Table 7.3, the coefficient, a, for the degraded areas is significantly larger than the saturated areas, and thus the degraded areas produce the majority of the sediment load. The agreement between observed and predicted sediment loads deteriorates rapidly if we increase the sediment concentration in the interflow from zero. Thus the simple model clearly demonstrates (Table 7.3) that most of the sediments originate from the degraded surface areas. Practically, these areas can be recognized easily in the

landscape during the growing season as the areas with little or no vegetation and not often farmed.
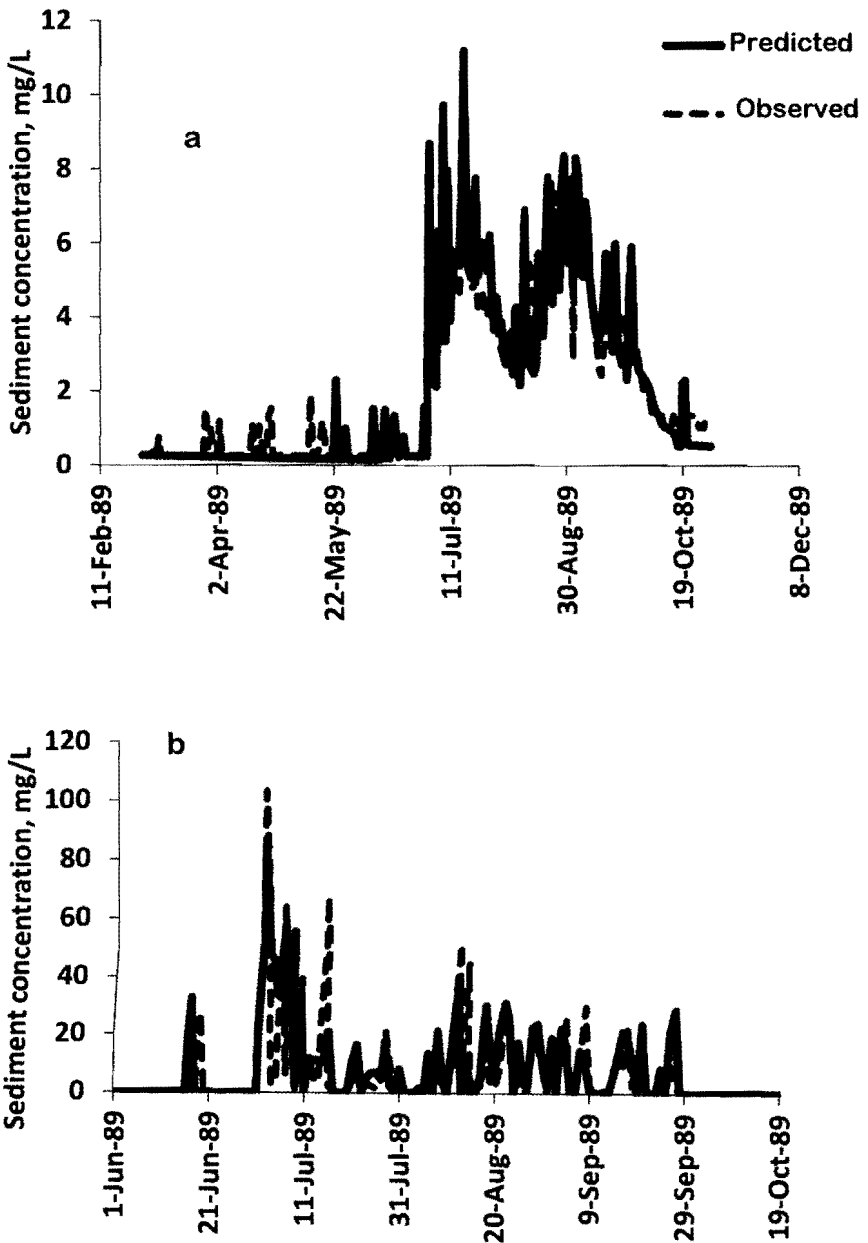

Figure 7.9 Predicted and observed (a) streamflow and (b) sediment concentration for the Anjeni watershed

Table 7.3 Model input parameters for the Anjeni watershed

Components	Description	Parameters	Unit	Calibrated values
Hydrology	Saturated area	Area A_s	%	2
		S_{max} in A_s	mm	70
	Degraded area	Area A_d	%	14
		S_{max} in A_d	mm	10
	Hillside	Area A_h	%	50
		S_{max} in A_h	mm	100
	Subsurface	BS_{max}	mm	100
	flow	$t_{1/2}$	days	70
	parameters	$\tau^\star$	days	10
Sediment	Saturated area	a_s	g l^{-1} (mm day^{-1})$^{-0.4}$	1.14
	Degraded area	a_d	g l^{-1} (mm day^{-1})$^{-0.4}$	4.70

Notes: A is fractional area for components of saturated area (s), degraded area (d) and hillside (h); S_{max} is maximum water storage capacity; $t_{1/2}$ is the time it takes in days to reduce the volume of the baseflow of the reservoir by a factor of 2 under no recharge condition; BSmax is maximum baseflow storage of linear reservoir; $\tau^\star$ is the duration of the period after a single rainstorm until interflow ceases; the constant a represents the sediment and watershed characteristics for the saturated area (s) and degraded areas (d) for obtaining the sediment concentration in the runoff

Soil and Water Assessment Tool

The Soil and Water Assessment Tool–Water Balance (SWAT-WB) model introduced in Chapter 6 allows us to study sediment losses for watersheds ranging from the micro-watershed (Anjeni) to the entire Ethiopian section of the Blue Nile (Easton *et al.*, 2010). Landscape erosion in SWAT is computed using the Modified Universal Soil Loss Equation (MUSLE), which determines sediment yield based on the amount of surface run-off. The SWAT-WB model improves the ability to correctly predict the spatial distribution of run-off by redefining the hydrologic response units (HRUs) by taking the topography into account and results in wetness classes that respond similarly to rainfall events. Thus by both predicting the run-off distribution correctly and using MUSLE the erosion from surface run-off producing areas is incorporated into the distributed landscape erosion predictions.

The robust SCRP data sets were used to calibrate and parameterize the SWAT-WB model (Easton *et al.*, 2010). The discharge in SWAT-WB model in Chapter 6 was calibrated using a priori topographic information and validated with an independent time series of discharge at various scales.

In Anjeni, the sediment hydrograph (Figure 7.10 and Table 7.4) has mimicked the flashy nature of the streamflow hydrograph. The fitting statistics were good for daily predictions (Table 7.4). For parameterization we assumed, in accordance with the SCRP watershed observation, that terraces have been utilized by approximately 25 per cent of the steeply sloped agricultural land to reduce erosion (Werner, 1986). To include this management practice, slope and slope length were reduced and the overland Mannings-n values were specified as a function of slope steepness (Easton *et al.*, 2010). Finally, Anjeni has a large gully providing approximately 25 per cent of the sediment (Ashagre, 2009). Since SWAT is incapable of realistically modelling gully erosion, the soil erodibility factor (USLE_K) in the MUSLE (Williams, 1975) was increased by 25 per cent to reflect this.
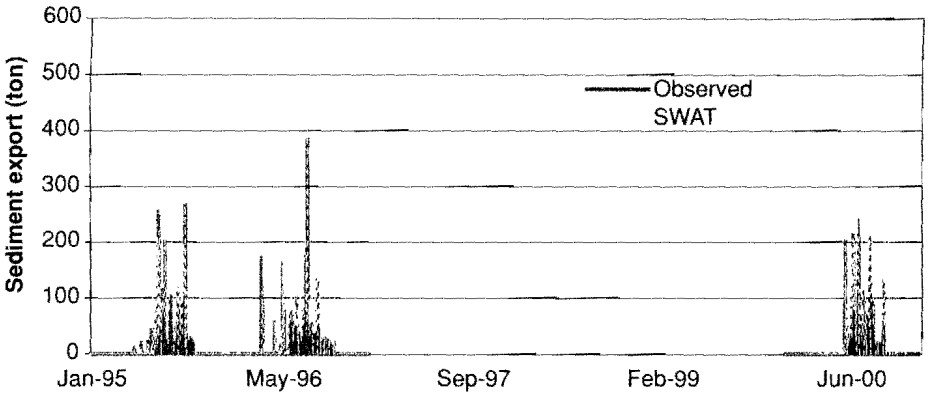
Figure 7.10 Measured and Soil and Water Assessment Tool–Water Balance predicted sediment export from the Anjeni micro-watershed

Table 7.4 shows the statistics for the measured and predicted sediment export for the two other locations for which we had data available, El Diem at the border with Sudan and the Ribb. In these simulations, the most sensitive parameters controlling erosion in the watershed were those used for calculating the maximum amount of sediment that can be entrained during channel routing (Easton *et al.*, 2010). The daily Nash–Sutcliff Efficiency (NSE) factor for the simulation period for the watersheds was approximately 0.7, indicating acceptable model performance. Nearly 128 million t yr^{-1} were delivered during the 2 years of measurements (Ahmed, 2003), with a measured daily average during the rainy season of 1.22 million tonnes. The model predicted 121 million tonnes over the 2 years, with a daily average of 1.16 million tonnes during the rainy season. The average sediment concentration at El Diem was 3.8 g l^{-1}, while the model predicted a slightly higher concentration of 4.1 g l^{-1}. The higher concentration was somewhat counterbalanced by the slightly under-predicted flow. Despite this, model performance appears to be adequate. El Diem sediment export was much less flashy than that in the Anjeni watershed (compare Figures 7.10 and 7.11). While the total sediment export intuitively increases with basin size, the normalized sediment export (in t km^2) was inversely proportional to the basin size (Table 7.4). This is a direct result of the difference in the base-flow coefficients (Π_b) among the basins of various sizes (e.g. 0.47 for Anjeni to 0.84 for the border at El Diem) and is similar to what is predicted with the simple spreadsheet erosion model.

Table 7.4 Model fit statistics (coefficient of determination, r^2 and NSE), and daily sediment export for the Anjeni, Ribb, and border (El Diem) sub-basins during the rainy season

Sub-basin	r^2	NSE	Measured sediment export (t d^{-1})	Modelled sediment export (t d^{-1})	Modelled sediment export (t·km^2 d^{-1})
Anjeni	0.80	0.74	239	227	201.2
Ribb*	0.74	0.71	30.6 × 10^3	29.5 × 10^3	22.7
Border (El Diem)	0.67	0.64	1.23 × 10^6	1.23 × 10^6	7.1

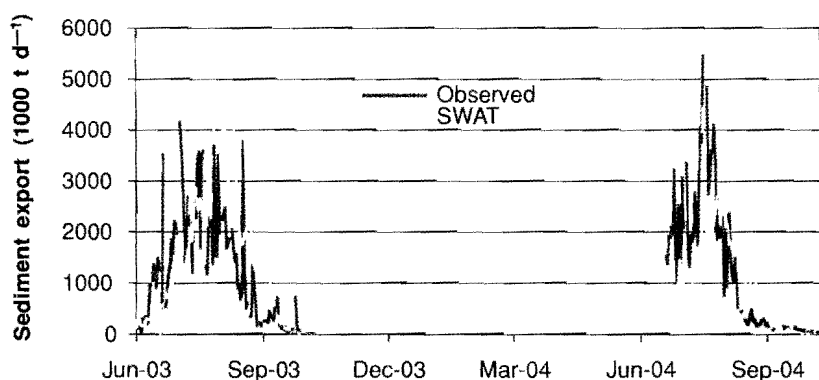*Note:* *Consists of four measurements

Figure 7.11 Observed and Soil and Water Assessment Tool–Water Balance modelled sediment export at the Sudan/Ethiopia border

Table 7.5 Annual predicted sediment yield for each wetness index class and for the pasture, crop and forest land covers. Wetness index one produces the lowest run-off and wetness class and ten the most

Land cover	Wetness index class sediment yield (t ha^{-1} yr^{-1})									
	One	Two	Three	Four	Five	Six	Seven	Eight	Nine	Ten
Pasture	1.2	3.6	3.4	3.6	3.9	5.6	8.8	10.1	12.5	14.3
Crop	2.1	2.3	3.4	3.5	4.6	5.9	10.7	9.9	14.2	15.6
Forest	0.3	0.5	0.9	1.5	1.7	1.6	2.8	3.1	3.7	4.1

Interestingly, the SAWT-WB model predicted that landscape-based erosion forms agricultural areas, particularly tilled fields in the lower slope positions which dominated sediment delivery to the river reaches during the early part of the growing season (approximately mid-end August), after which landscape-based erosion was predicted to decrease. The reduction in landscape-borne sediment reflects the growth stages of plants in the highlands, which in mid-late August are reasonably mature, or at least have developed a canopy and root system that effectively reduce rill and sheet erosion (Zegeye *et al.*, 2010). The reduction of sediment load can also be caused by a stable rill network (resulting in very little erosion losses) that is established once the fields in the watershed are not ploughed anymore. The plant cover is a good proxy for this phenomenon since the fields with plants are not ploughed. After the upland erosion stops, the sediment export from the various sub-basins is controlled by channel erosion and re-entrainment/resuspension of landscape sediment deposited in the river reaches in the early part of the growing season. This sediment is subsequently mobilized during the higher flows that typically peak after the sediment peak is observed (e.g. the sediment peak occurs approximately 2 weeks in July, before the flow peaks in August). This, of course, has implications for reservoir management in downstream countries in that much of the high sediment flow can pass through the reservoir during the rising limb, and the relatively cleaner flows stored during the receding limb. Nevertheless, the sheer volume of sediment exported from the Ethiopian Highlands

threatens many downstream structures regardless of their operation, and clearly impacts agricultural productivity in the highlands.

Predicting spatial distribution of erosion

Predicting the spatial distribution of run-off source areas is a critical step in improving the ability to manage landscapes such as the Blue Nile to provide clean water supplies, enhance agricultural productivity and reduce the loss of valuable topsoil.

Using the validated SWAT-WB model, the predicted gradient in sediment yield within sub-basins is illustrated in the inset of Figure 7.12, where the Gumera watershed in the Lake Tana sub-basin is shown. The model predicts only a relatively small portion of the watershed to contribute the bulk of the sediment (75% of the sediment yield originates from 10% of the area) while much of the area contributes low sediment yield. The areas with high sediment yield are generally predicted to occur at the bottom of steep agricultural slopes, where sub-surface flow accumulates, and the stability of the slope is reduced from tillage and/or excessive livestock traffic. Indeed, Table 7.5 shows that these areas (higher wetness index classes or areas with higher λ values) inevitably produce substantially higher sediment yields than other areas as the latter produce higher run-off losses as well. This seems to agree with what has been observed in the basin (e.g. Tebebu *et al.*, 2010), and points towards the need to develop management strategies that incorporate the landscape position into the decision-making process. Interestingly, both pastureland and cropland in the higher wetness classes had approximately equivalent sediment losses, while the forests in these same areas had substantially lower erosive losses, likely due to the more consistent ground cover and better root system.
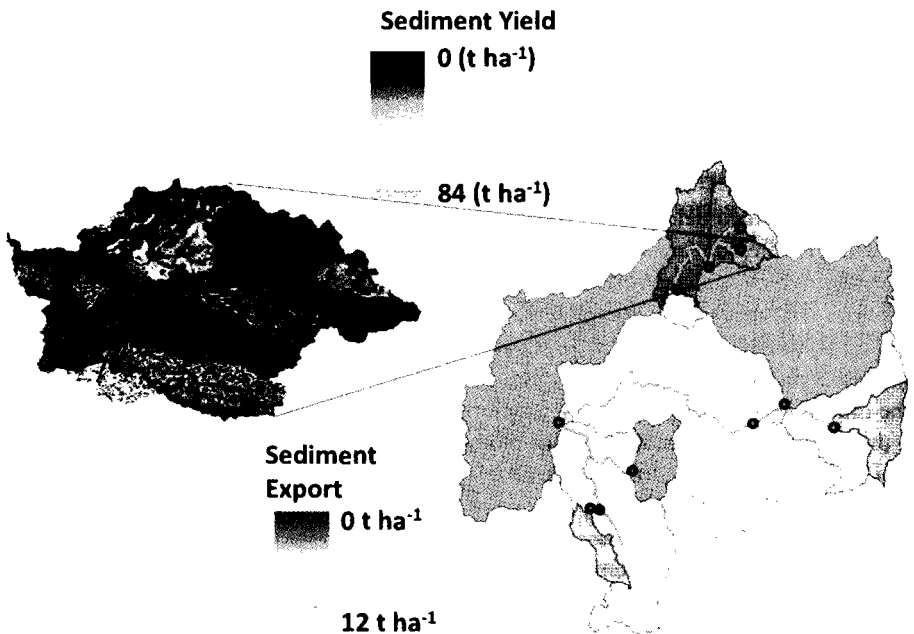

Sediment Yield

0 (t ha⁻¹)

84 (t ha⁻¹)

Sediment Export

0 t ha⁻¹

12 t ha⁻¹

Figure 7.12 Sediment export (t ha⁻¹ yr⁻¹) in the sub-basins predicted by the SWAT-WB model (main figure) and sediment yield by hydrologic response unit (HRU) for the Gumera sub-basins (inset)

Spatial distribution of sediment in the Gumera watershed (east of Lake Tana) simulated by Betrie *et al.* (2009) with the original infiltration-excess-based SWAT-CN model is shown in Figure 7.13. A comparison with the saturation-excess-based, SWAT-WB model (inset in Figure 7.12) shows that the amounts of sediment and its distribution are different. Although the sediment leaving the watershed might not be that different, the location where soil and water conservation practices have the most effect is quite different.
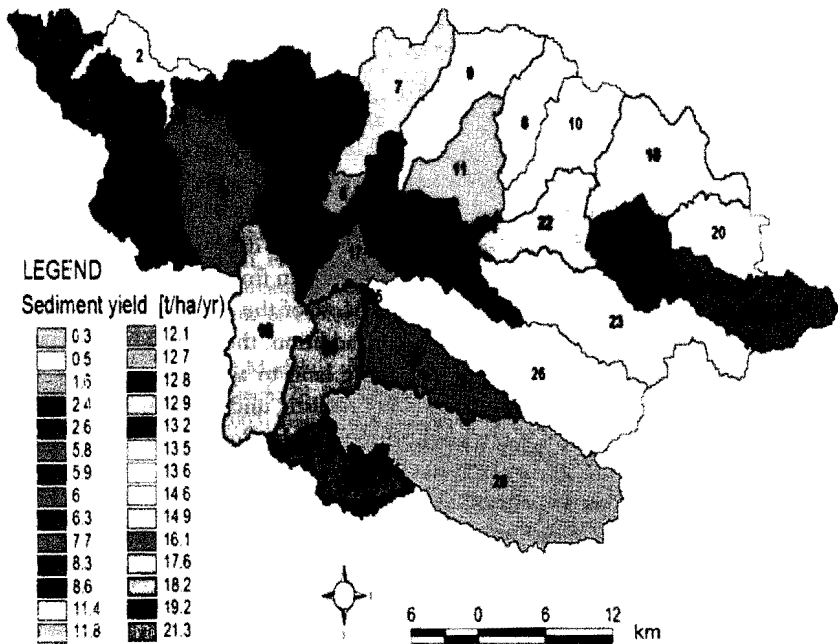

Figure 7.13 Spatial distribution of average annual sediment yield by sub-watershed (t ha^{-1} yr^{-1}) simulated using SWAT

Note: 1–29 are sub-watershed numbers in the Gumera watershed

Obviously, in addition, the erosion routines (USLE, RUSLE, MUSLE, sediment rating curves) in many of the large-scale watershed models are crude at best, and do not incorporate the appropriate mechanistic processes to reliably predict when and where erosion occurs, at least at the scale needed to manage complex landscapes. For instance, the MUSLE routine in SWAT does not predict gully erosion, which is a large component of the sediment budget in the Blue Nile. To correctly capture the integrated watershed-wide export of sediment, the original SWAT model predicts erosion to occur more or less equally across the various land covers (e.g. cropland and pastureland produce approximately equal erosive losses provided they have similar soils and land management practices throughout the basin). The modified version of SWAT used here recognizes that different areas of a basin (or landscape) produce differing run-off losses and thus differing sediment losses (Table 7.5). However, all crops or pastures

within a wetness index class in the modified SWAT produce the same erosive losses, rill or sheet erosion (as predicted by MUSLE), but not the same gully erosion. Thus, rill and sheet erosion are likely over-predicted to obtain the correct sediment export from the basin.

Concluding remarks

Erosion, sediment transport and sedimentation of reservoirs are critical problems in the BNB. The current levels of erosion are causing irreversible levels of soil degradation and loss of livelihoods and are already resulting in significant costs in canal and reservoir dredging or in heightening plans of reservoirs. The BNB, while providing significant flow, also contributes substantial sediment loads. The analysis of data at various scales shows that the seasonal sediment distribution is highly variable, and that the highest sediment concentration occurs in July, when most of the land is cultivated, leading to significant loss of soil and nutrients from agricultural fields. The consequence is rapid accumulation (of sediment) and loss of capacity of small reservoirs built for agricultural or other water supplies and rapid filling of the dead storage of large reservoirs and natural and man-made lakes.

The major implication of this chapter is that erosion is distributed through the watershed. By incorporating management practices to reduce erosion from areas that generate most of the run-off, sedimentation in rivers can be reduced. Most of the erosion occurs in the areas with degraded soils or limited infiltration capacity. In addition, the saturated areas can potentially contribute sediment when converted from grazing land to agricultural land where crops are grown after the wet season. This, of course, is not realistic under the present economic conditions but could be considered if some kind of payment by downstream beneficiaries is made. According to unofficial data, 70 per cent of the cost of operation and maintenance (O&M) in the Blue Nile part of Sudan is spent on sediment-related canal maintenance.

The utility of vegetative filters in providing a significant reduction in the sediment load to the upper Blue Nile has been demonstrated in a study by Tenaw and Awulachew (2009). Application of the vegetative filter and other soil and water conservation interventions throughout the basin could help to reverse land degradation and improve the livelihoods of the people upstream, and at the same time reduce the cost of O&M of hydraulic infrastructure and sedimentation damage downstream. In order to target the critical areas requiring interventions, more fieldwork and model validation are required on the exact locations of the high erosion-risk areas.

References

Abiy, A. Z. (2009) Geological controls in the formations and expansions of gullies over hillslope hydrological processes in the Highlands of Ethiopia, northern Blue Nile region, MPS thesis, Cornell University, Ithaca, NY.

Ahmed, A. A. (2003) *Towards Improvement of Irrigation Systems Management*, AMCOW Conference, Addis Ababa, Ethiopia.

Ahmed, A. A. and Ismail, U. H. A. E. (2008) *Sediment in the Nile River System*, UNESCO/IHP/International Sediment Initiative, www.irtces.org/isi/isi_document/Sediment%20in%20the%20Nile%20River%20 System.pdf, accessed 27 October 2011.

Ashagre, B. B. (2009) SWAT to identify watershed management options: Anjeni watershed, Blue Nile basin, Ethiopia, MPS thesis, Cornell University, Ithaca, NY.

Awulachew, S. B., McCartney, M., Steenhuis, T. S. and Ahmed, A. A. (2008) *A Review of Hydrology, Sediment and Water Resource Use in the Blue Nile Basin*, Working Paper 131, IWMI, Colombo, Sri Lanka.

Bashar, K. E and Khalifa, E. A. (2009) Sediment accumulation in the Roseires reservoir, in *Improved Water and Land Management in the Ethiopian Highlands: Its Impact on Downstream Stakeholders Dependent on the Blue*

Nile, Intermediate Results Dissemination Workshop held at the International Livestock Research Institute (ILRI), Addis Ababa, Ethiopia, 5–6 February, International Water Management Institute, Colombo, Sri Lanka, http://publications.iwmi.org/pdf/H042510.pdf, accessed 17 August 2011.

Bayabil, H. K., Tilahun, S., Collick, A. S., Yitaferu, B. and Steenhuis, T. S. (2010) Are run-off processes ecologically or topographically driven in the (sub)humid Ethiopian highlands? The case of the Maybar watershed, *Ecohydrology*, 3, 4, 457–466.

Betrie, G. D., Mohamed, Y. A., van Griensven, A., Popescu, I. and Mynett, A. (2009) Modeling of soil erosion and sediment transport in the Blue Nile Basin using the open model interface approach, in *Improved Water and Land Management in the Ethiopian Highlands: Its Impact on Downstream Stakeholders Dependent on the Blue Nile*, Intermediate Results Dissemination Workshop held at the International Livestock Research Institute (ILRI), Addis Ababa, Ethiopia, 5–6 February, International Water Management Institute, Colombo, Sri Lanka, http://publications.iwmi.org/pdf/H042513.pdf, accessed 17 August 2011.

Bewket, W. and Sterk, G. (2005) Dynamics in land cover and its effect on stream flow in the Chemoga watershed, Blue Nile basin, Ethiopia, *Hydrological Process*, 19, 445–458.

Capra, A., Mazzara, L. M. and Scicolone, B. (2005) Application of EGEM model to predict ephemeral gully erosion in Sicily, Italy, *Catena*, 59, 133–146.

Easton, Z. M., Fuka, D. R., White, E. D., Collick, A. S., McCartney, M., Awulachew, S. B., Ahmed, A. A. and Steenhuis, T. S. (2010) A multi basin SWAT model analysis of run-off and sedimentation in the Blue Nile, Ethiopia, *Hydrology and Earth System Sciences*, 14, 1827–1841.

FAO (Food and Agriculture Organization of the United Nations) (1986) *Highlands Reclamation Study: Ethiopia*, Final Report, vols I and II, FAO, Rome, Italy.

Guzman, C. (2010) Suspended sediment concentration and discharge relationships in the Ethiopian Highlands, MS thesis, Department of Biological and Environmental Engineering Cornell University, Ithaca, NY.

Hairsine, P. B. and Rose, C. W. (1992) Modeling water erosion due to overland flow using physical principles 1. Sheet flow, *Water Resources Research*, 28, 1, 237–243.

Haregeweyn, N. and Yohannes, F. (2003) Testing and evaluation of the agricultural non-point source pollution model (AGNPS) on Augucho catchment, western Hararghe, Ethiopia, *Agriculture Ecosystems and Environment*, 99, 1–3, 201–212.

Herweg, K. (1996) *Field Manual for Assessment of Current Erosion Damage*, Soil Conservation Research Programme (SCRP), Ethiopia and Centre for Development and Environment (CDE), University of Berne, Berne, Switzerland.

Hurni, H., Kebede, T. and Gete, Z. (2005) The implications of changes in population, land use, and land management for surface run-off in the upper Nile basin area of Ethiopia, *Mountain Research and Development*, 25, 2, 147–154.

Hydrosult Inc., Tecsult, DHV and their Associates Nile Consult, Comatex Nilotica and T and A Consulting (2006) *Trans-Boundary Analysis: Abay-Blue Nile Sub-basin*, Nile Basin Initiative-Eastern Nile Technical Regional Organization (NBI-ENTRO), Addis Ababa, Ethiopia.

Kaltenrieder, J. (2007) *Adaptation and Validation of the Universal Soil Loss Equation (USLE) for the Ethiopian-Eritrean Highlands*, Diplomarbeit der Philosophisch-Naturwissenschaftlichen Fakultät der Universität Bern, Centre for Development and Environment Geographisches www.cde.unibe.ch/CDE/pdf/Kaltenrieder%20Juliette_USLE%20MSc%20Thesis.pdf, accessed 17 August 2011.

Mitiku, H., Herweg, K. and Stillhardt, B. (2006) *Sustainable Land Management – a New Approach to Soil and Water Conservation in Ethiopia*, Land Resource Management and Environmental Protection Department, Mekelle University, Mekelle, Ethiopia, Center for Development and Environment (CDE), University of Bern and Swiss National Center of Competence in Research (NCCR) North-South, Bern, Switzerland.

Mohamed, Y. A., Bastiaanssen, W. G. M. and Savenije, H. H. G. (2004) Spatial variability of evaporation and moisture storage in the swamps of the upper Nile studied by remote sensing techniques, *Journal of Hydrology*, 289, 1–4, 145–164.

Nyssen, J., Poesen, J., Moeyerson, J. and Mitiku Haile Deckers, J. (2008) Dynamics of soil erosion rates and controlling factors in the Northern Ethiopian Highlands – towards a sediment budget, *Earth Surface Processes and Landforms*, 33, 5, 695–711.

Nyssen, J., Poesen, J., Veyret-Picot, M., Moeyersons, J., Mitiku Haile Deckers, J., Dewit, J., Naudts, J., Kassa Teka and Govers, G. (2006) Assessment of gully erosion rates through interviews and measurements: a case study from Northern Ethiopia, *Earth Surface Processes and Landforms*, 31, 2, 167–185.

Setegn, S. G., Srinivasan, R. and Dargahi, B. (2008) Hydrological modelling in the Lake Tana Basin, Ethiopia using SWAT model, *The Open Hydrology Journal*, 2, 24–40.

Tebebu, T.Y., Abiy, A. Z., Zegeye, A. D., Dahlke, H. E., Easton, Z. M., Tilahun, S. A., Collick, A. S., Kidnau, S., Moges, S., Dadgari, F. and Steenhuis, T. S. (2010) Surface and subsurface flow effect on permanent gully formation and upland erosion near Lake Tana in the Northern Highlands of Ethiopia, *Hydrology and Earth System Sciences*, 7, 5235–5265.

Tenaw, M. and Awulachew, S. B. (2009) *Soil and Water Assessment Tool (SWAT)-Based Runoff and Sediment Yield Modeling: A Case of Gumera Watershed in Lake Tana Subbasin*, http://home.agrarian.org:8080/ethiopia%20work%20frank/vertisols/ethiopian%20%20soils/H042511.pdf, accessed 26 April 2012.

Tilahun, S. A., Guzman, C. D., Zegeye, A. D., Sime, A., Collick, A. C., Rimmer, A. and Steenhuis, T. S. (2012) An efficient semi-distributed hillslope erosion model for the sub-humid Ethiopian Highlands, *Hydrological Earth System Sciences Discussions*, 9, 2121–2155.

Werner, C. (1986) *Soil Conservation Experiments in the Anjeni Area*, Gojam Research Unit (Ethiopia), Institute of Geography, University of Bern, Bern, Switzerland.

Williams, J. R. (1975) *Sediment – Yield Prediction with Universal Equation Using Runoff Energy Factor*, Proceedings of the Sediment-Yield Workshop, USDA Sedimentation Laboratory, Oxford, MS.

Zegeye, A. D., Steenhuis, T. S., Blake, R. W., Kidnau, S., Collick, A. S. and Dadgari, F. (2010) Assessment of upland erosion processes and farmer perception of land conservation in Debre-Mewi watershed, near Lake Tana, Ethiopia, presented at Ecohydrology for water ecosystems and society in Ethiopia, International Symposium, 18–20 November, Addis Ababa, Ethiopia.

Zeleke, G. (2000) *Landscape Dynamics and Soil Erosion Process Modeling in the North-Western Ethiopian Highlands*, African Studies Series A 16, Geographica Bernensia, Berne, Switzerland.